Mario Anton Schriefl

An Investigation of Electron Beam Induced Deposited Platinum Discs as Schottky Contacts

Bachelor Thesis

For obtaining the academic degree
Bachelor of Science

Bachelor Program of Technical Physics

Supervisor:
Univ.-Prof. Peter Hadley
Institute of Solid State Physics

Graz, August 13, 2012

Acknowledgement

I want to thank my supervisor Univ.-Prof. Ph.D. Peter Hadley for giving me the possibility to write this bachelor thesis in a way, where I learned very much about scientific work. I want to acknowledge him for the large amount of time he spent for supporting my work. Futhermore I want to thank Stefan Kirnstötter and Martin Faccinelli for helping me with the measurements and for lots of other things they did for me all along the project.

Contents

1 Abstract 4

2 Motivation 4

3 Measurement Methods 5
3.1 Used Equipment 5
3.2 EBIC – Electrion Beam Induced Current 5
3.3 4-Point Resistivity Measurements 7
3.4 IV measurements 15

4 Investigated Samples 16
4.1 Platinum Sample 16
4.2 EMCON Diode 18

5 Results 20
5.1 EBIC Measurements on the Platinum Sample 20
5.2 Resistance of the Platinum 24
5.3 Stability of the Contacts 27
5.4 IV Curves 28

6 Conclusions 30

7 Suggestions 31

1 Abstract

Electrical measurements with sharp tips can be used to locally determine the materials properties of conductors. This is especially important for semiconductor devices where properties such as the resistivity, the carrier density, the mobility, the diffusion length, and the minority carrier lifetime vary as a function of position throughout the device. In this project, 4-point resistivity measurements and Electron Beam Induced Current (EBIC) measurements were used to measure the resistivity and minority carrier diffusion length in silicon power devices. One of the difficulties with these measurements is that the contact between the metal tips and the silicon is not reproducible and often fluctuates in time. To try to produce more stable contacts, platinum discs were deposited on the silicon by Electron Beam Induced Deposition (EBID). The properties of the platinum contacts were compared to the contact formed by just placing tungsten tips on the silicon.

2 Motivation

In a collaboration between TU Graz and Infineon, semiconductor power devices are being studied. They are used as switchers or rectifiers in high-voltage or high-current applications (e.g. in the automobile or the train industries). To ensure that the device doesn't get damaged (e.g. because of high voltages) sometimes it is necessary to use low doping concentrations. In such cases defects play an important role in determining the carrier concentration. At low doping concentrations, it is difficult to determine properties like the resistivity or the carrier density exactly. To complement determination of the resistivity that is performed at Infineon using spreading resistance measurements [9], 4-point measurements and EBIC measurements are performed at the TU Graz.

For the 4-point and EBIC measurements, sharp tungsten needles were put on the surface of the semiconductor. There are different problems with these contacts such as the contact stability. To make a stable contact you have to put the tip with the right pressure on the probed surface. If the pressure is too low, the contact is not useful. Too high pressure often leads to bended tips with the consequence, that the exact contact position is not known [11]. Another problem is, that the Schottky contact is not reproducible because it is not possible to control the movement of the micromanipulators (they hold the tips cf. section 3.1) as well as necessary. Also problematic is the small area of the contacts (about $10\,\mathrm{nm}^2$) which leads to fluctuations.
So the idea to do this bachelor thesis was to make larger contacts with a defined contact area of about $10\,\mu\mathrm{m}^2$. Therefore platinum discs were put on the cross section of the semiconductor by Electron Beam Induced Deposition [4]. This increases the contact area by a factor of 10^6 and we hoped for a corresponding decrease in the contact resistance.

With the assumption that the platinum is a good conductor with a homogeneous resistivity, for the EBIC measurements (cf. section 5.1) we had expected, that there is no EBIC current measured through the structures. That especially applies to low acceleration voltages, because at the platinum regions electron-hole pairs can't be generated if the electron beam has too low energy for penetrating the platinum. (cf. section 3.2)

To make an investigation of the homogeneity of the platinum we had planned a measurement between two tips landed on two platinum discs in which they are connected by a platinum line. So we wanted to get informations about the deposited material, as there are the electrical behavior (metal or insulator) or the resistance.

3 Measurement Methods

3.1 Used Equipment

For the measurements a JEOL 6490 LV SEM (Scanning Electron Microscope) was used. Inside the SEM four Kleindiek micromanipulators holding thin tungsten tips were employed to put the thin tips on the cross section of the investigated sample. The manipulators were steered by a Playstation Controller. Furthermore the probed sample was mounted in a sample-holder, which contacted it perpendicular to the cross section. These contacts of the coppery sample-holder we called edge contacts of the sample. The edge contacts, and also the tungsten tips, were attached to BNC connectors on a flange of the SEM. To ensure that the tips touch the sample surface with the right pressure, we used an automatic landing program. This program moves the tip downwards while the current flowing between the tip and the wafer is measured. If this current exceeds a certain value, the movement is stopped. Nevertheless it was difficult to land the tip on a defined small area due to the stick slip motion of the micromanipulators [2]. The SEM was connected with a PC, which ran a program for the SEM. With that program all settings regarding to the microscope could be made, such as the acceleration voltage or the magnification. With the program we were also able to see the movements of the tungsten needles.

3.2 EBIC – Electrion Beam Induced Current

At a pn-junction (contact of a n-doped and a p-doped region) an electric field results, whose magnitude depends on the doping concentrations. Almost the same thing occurs

at the contact of a metal and a semiconductor (Schottky contact [16]). Due to this built-in electric field, charge carriers in the surrounding begin to move. If an electron beam hits a semiconductor, electron-hole pairs are generated. It's almost the same process, which occurs when light impinges on a solar cell (cf. [14]). Because of the build-in electric field the charge carriers begin to move and a current flows without a biased voltage. This EBIC current is much higher than the emission current (current, which comes from the e-beam and flows through the grounded sample [5]) because each of the electrons of the e-beam has a high enough energy (a few keV) to generate a large amount of electron-hole pairs. If the EBIC current was in the order of the specimen current, the EBIC pictures would have no meaningfulness. If for example a metal tip touches the surface of a semiconductor and the sample itself is connected with the tip over an amperemeter, the electric field of that Schottky contact causes a current, which can be measured. Furthermore because the charge carriers have a certain diffusion length in the semiconductor, the detected current will be higher if the generated electron-hole pairs (and so the e-beam) are close to the Schottky contact. If the charge carriers are far away from the Schottky contact, most of them will recombine before they come to the contact, so the EBIC current will be lower.
For our measurements we used a SEM (Scanning Electron Microscope) which generated the electron beam and moved it over the surface of the investigated sample. You can see a typical EBIC measurement in figure 1, where a tungsten tip is positioned on the cross section of a p-doped silicon wafer. Moreover there is a general rule, with that you can determine the kind of doping of the sample, which says that if the signal on the measuring electrode (in that case the tungsten tip) is negative, the sample is p-doped. If the signal is positive, it is n-doped.

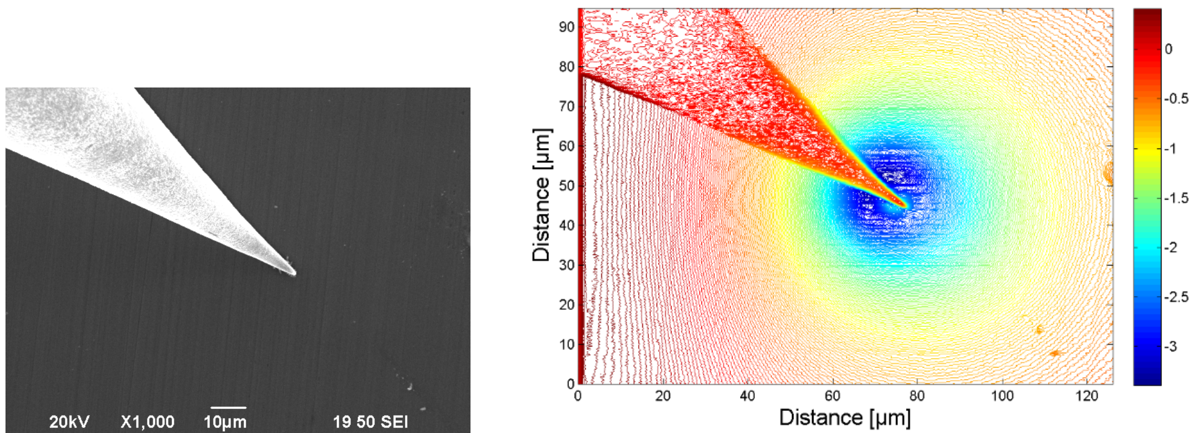

(a) Accompanying SEM picture with an amplification of 1000 and an acceleration voltage of 20 kV.

(b) 2D-map from the EBIC scan: the current which flows through the tip is measured as a function of position.

Figure 1: EBIC measurement between a tungsten tip and a p-doped silicon wafer

3.3 4-Point Resistivity Measurements

To investigate the resistivities of semiconductor power devices the resistance of different regions on the cross section of the probed wafer has to be measured. The common way to measure the resistance is to put two contacts on the sample. These contacts are connected with an ohmmeter which measures the resistance. This resistivity of the sample can be calculated with $R_S = \rho \cdot \frac{\mathrm{l}}{\mathrm{A}}$, where l is the distance between the contacts, A is area which is suffused by the measuring current, and ρ is the resistivity. For the resistance measurements of semiconductor power devices two metal needles landed on the probed surface act as measuring contacts. By measuring the resistance in that way aside from the sample resistance also the resistances of the contacts and the connection cables are measured. Since the cables are usually made of copper, that resistance can be ignored.

In figure 2 the situation for the 2-point measurement is shown. The Voltage, measured between the two contacts is given by $V = I\,(R_{C1} + R_{C2} + R_S)$. So the condition for a useful measurement is, that the two contact resistances have to be much smaller than the sample resistance. $(R_{C1} + R_{C2} \ll R_S)$
But it is difficult to comply with that condition because, as mentioned in section 2, the contact resistances could be problematic since it's difficult to get stable, reproducible contacts and also the small contact area can be a problem.

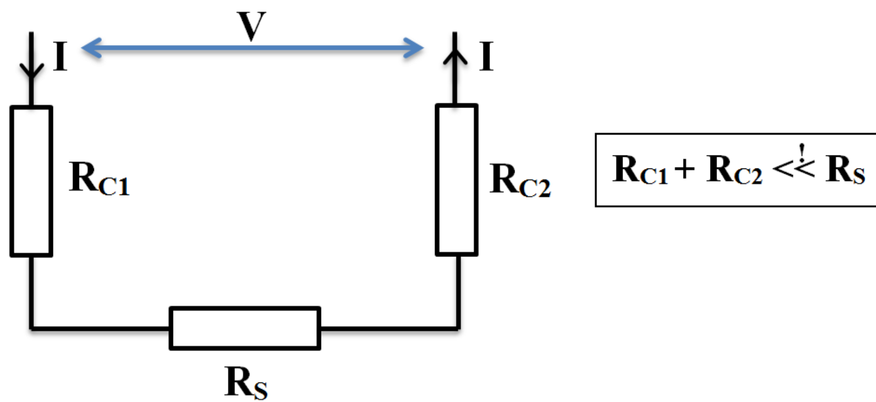

Figure 2: 2-point Measurement: The diagram of connections shows the two contact resistances R_{C1} and R_{C2} and the sample resistance R_S. These three resistances are connected in series, the measuring current I flows through all of them.

Due to that difficulties it's convenient to use a 4-point configuration, where a measuring current is flowing from the first contact through the sample to the second one, and the voltage is measured between the 3rd and the 4th contact. As shown on [3], the sample resistance can be determined by dividing the measured voltage by the applied current.

The diagram of connections of the 4-point configuration can be seen in figure 3. By considering the inner circuit (circuit of the measured voltage), we see, that the voltage measured from the voltmeter and the voltage across the sample are not the same. We can write the following equations:

$$V_M = I_M \cdot (R_{C3} + R_{C4}) + V_S$$
$$V_S = V_M - \tfrac{V_M}{R_M}\,(R_{C3} + R_{C4})$$
$$V_S = \left(1 - \tfrac{R_{C3}+R_{C4}}{R_M}\right) \cdot V_M$$
$$\Rightarrow \qquad \underline{R_{C3} + R_{C4} \ll R_M}$$

Now to make a useful measurement, the contact resistances R_{C3} and R_{C4} have to be much smaller than R_M. So also the voltage contacts should have a small resistance. The contact resistances also depends on the contact area. If the contact area is small, the contact resistance increases (cf. equation 15).

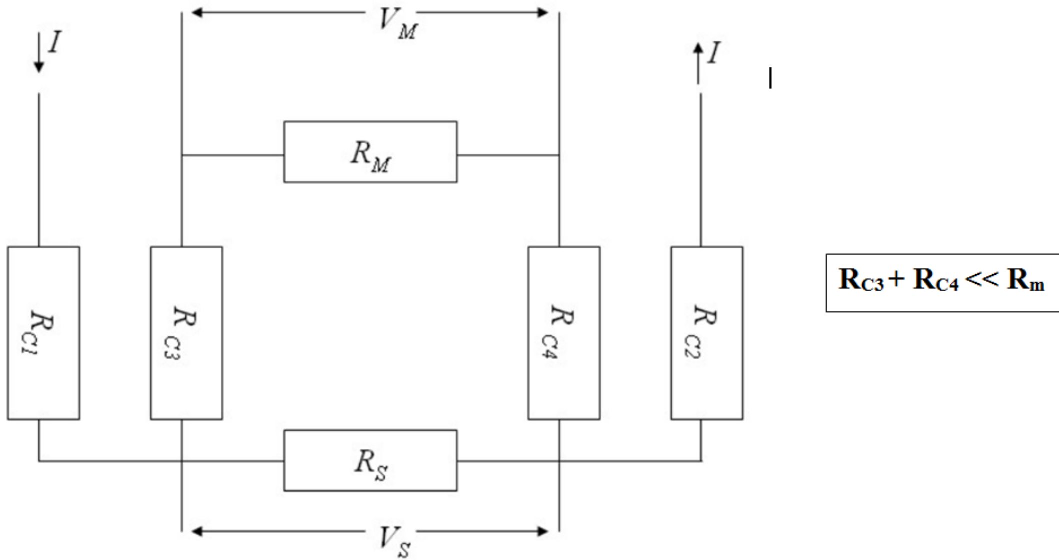

Figure 3: 4-point Measurement: The diagram of connections shows the four contact resistances R_{C1}, R_{C2}, R_{C3} and R_{C4}, the sample resistance R_S and the equivalent resistance of the voltmeter R_M. The measuring current I flows into the first contact (R_{C1}) and comes out at the second one (R_{C2}). There is another current I_M, which is applied by the voltmeter to measure the voltage V_M. V_S is the voltage across the sample. (The picture is copied from [3])

On the webpage [3] the calculation of the 4-point resistivity measurement can be seen. There it is shown how to determine the resistivity of the sample if you know the contact

positions, the applied current and the measured voltage. In the used calculation model it was assumed, that the current distribution on a contact is radial symmetric. For a probe with a homogeneous resistivity the measured resistance should be independent from how big the distance is between the measuring tips. It turns out, that this model works good for low sample resistivities, but for high sample resistivities it doesn't. Furthermore that model doesn't work well when the current tips are put beside an interface of two different doping regions or in the near of the edge of the sample. In such cases it's necessary to work with additional image current sources. And there was also a small dependence of the measuring tip distances registered.

Now the idea was, to evolve a 4-point model for well defined round metal discs, as we wanted to have on our platinum sample. For that model we considered the contact in oblate spheroidal coordinates (see figure 4), like Maxwell did it in his calculation (cf. [12]). We assumed, that the current flows through round metal discs in the way like Maxwell described. He solved the Laplace equation in these coordinates and came to the solution, that the contact resistance $R_{Maxwell} = \frac{\rho}{2a}$, where ρ is the resistivity of the contact and a is the radius of the round contact.
Maxwall got this easy solution by solving an electrostatic problem. We wanted to verify his calculations to find an electrostatic potential, which solves the Laplace equation. Because if we would know the electrostatic potential, we could calculate the electric field, the current density and the current, which flows through the current contacts. Moreover we would be able to write the measured voltage as differences of the electrostatic potential treated from the current contacts.

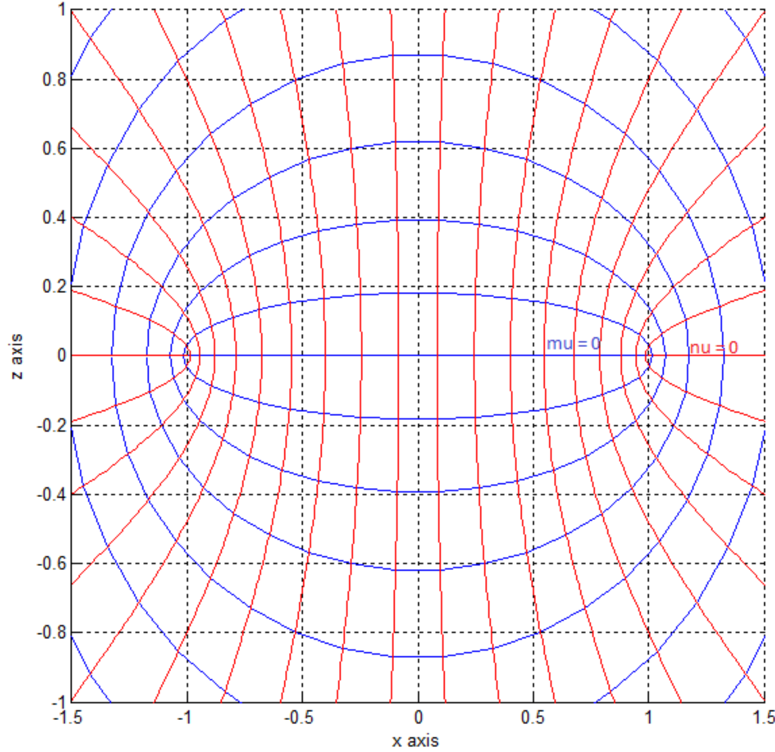

Figure 4: Oblate spheroidal coordinates in the x-z-plane: the blue lines are the lines of constant μ-values, the red lines are lines of constant ν-values. Considered in the z=0-plane $\mu = 0$ inside the focal ring and $\nu = 0$ outside the focal ring. The radius of the focal ring, which looks like a circle in the z=0-plane, is a.

The transformation equations for the oblate spheroidal coordinates are:

$$x = a\cosh\mu\cos\nu\cos\phi \qquad y = a\cosh\mu\cos\nu\sin\phi \qquad z = a\sinh\mu\sin\nu \tag{1}$$

As first step we verified the calculations of Maxwell, so we solved the Laplace equation in oblate spheroidal coordinates where the Laplacian is

$$\nabla^2\Phi = \frac{1}{a^2\left(\sinh^2\mu+\sin^2\nu\right)}\left[\frac{1}{\cosh\mu}\frac{\partial}{\partial\mu}\left(\cosh\mu\frac{\partial\Phi}{\partial\mu}\right)+\frac{1}{\cos\nu}\frac{\partial}{\partial\nu}\left(\cos\nu\frac{\partial\Phi}{\partial\nu}\right)\right]+\frac{1}{a^2\left(\cosh^2\mu+\cos^2\nu\right)}\frac{\partial^2\Phi}{\partial\phi^2}.$$

We want to find an expression for the electrostatic potential. Due to the fact that the result of Maxwell looks very easy, we guess that also the potential cannot be a very complicate expression. So we assume, that the Φ only depends on μ. Then,

$$\frac{d}{d\mu}\left(\cosh\mu\frac{d\Phi}{d\mu}\right) = 0. \tag{2}$$

This can be written as,

$$\cosh \frac{d^2\Phi}{d\mu^2} = -\sinh \mu \frac{d\Phi}{d\mu}. \tag{3}$$

We substitute $y(\mu) = \frac{d\Phi}{d\mu}$

$$\frac{dy}{d\mu} = -\tanh \mu \cdot y \tag{4}$$

We solve that equation by the separation of variables.

$$\frac{dy}{y} = -\tanh \mu \cdot d\mu \tag{5}$$

After integration, this is

$$\ln y = -\ln(\cosh \mu) + c_1 \qquad \Rightarrow \qquad y = \frac{\exp(c_1)}{\cosh \mu} = \frac{d\Phi}{d\mu}. \tag{6}$$

Another integration yields

$$\Phi = 2 \cdot \exp(c_1) \cdot \tan^{-1}\left(\tanh \frac{\mu}{2}\right) + c_2. \tag{7}$$

Since it is always possible to add a constant to the solution, we can set $c_2 = 0$. The term $\tan^{-1}\left(\tanh \frac{\mu}{2}\right)$ goes to $\frac{\pi}{4}$ if μ goes to infinity. If some voltage $V/2$ is applied on one side of the contact for very large μ and $-V/2$ is applied on the other side of the contact for large μ then the potential that fulfills these boundary conditions is given by,

$$\boxed{\Phi = \frac{2V}{\pi} \cdot \tan^{-1}\left(\tanh\left(\frac{\mu}{2}\right)\right), \qquad 0 \le \mu < \infty} \tag{8}$$

This is V/2 for $\mu = \infty$.

Here V is the voltage applied across the contact (e.g. from +z to −z), so it can be written as $V = R \cdot I$, where R is the contact resistance and I is the measuring current, which flows through the contact. To be sure, that the expression (8) for the electrostatic potential is correct, we check it by putting the potential into the Laplace equation $\nabla^2\phi = 0$, which is given by equation (2), because Φ only depends on μ:

- $\frac{\partial \Phi}{\partial \mu} = \frac{V}{\pi} \cdot \mathrm{sech}\mu$
- $\frac{\partial}{\partial \mu}\left[\frac{V}{\pi} \cdot \cosh \mu \cdot \mathrm{sech}\mu\right] = 0, \quad$ because $\quad \mathrm{sech}\mu = \frac{1}{\cosh \mu}$

So now we can calculate the electric field by calculating the gradient of the potential, $\mathbf{E} = -\nabla\Phi$. Here we can also work only with the μ-part of the nabla operator:

$$\mathbf{E} = -\frac{\hat{\mathbf{e}}_\mu}{a\sqrt{\sinh^2\mu + \sin^2\nu}}\frac{\partial}{\partial\mu}\Phi, \quad \hat{\mathbf{e}}_\mu = \frac{1}{\sqrt{\sinh^2\mu + \sin^2\nu}}\begin{pmatrix}\sinh\mu\cos\nu\cos\varphi \\ \sinh\mu\cos\nu\sin\varphi \\ \cosh\mu\sin\nu\end{pmatrix} \tag{9}$$

$$\Rightarrow \mathbf{E} = -\frac{V\mathrm{sech}\mu}{a\pi\sqrt{\sinh^2\mu + \sin^2\nu}}\hat{\mathbf{e}}_\mu \tag{10}$$

Using $\mathbf{j} = \sigma\mathbf{E}$ we can calculate the current density (σ is the conductivity)

$$\Rightarrow \mathbf{j} = -\frac{\sigma V}{a\pi}\frac{\mathrm{sech}\mu}{\sqrt{\sinh^2\mu + \sin^2\nu}}\hat{\mathbf{e}}_\mu \tag{11}$$

The current density is symmetric with respect to rotation around the z-axis. Now we want to calculate the current, that flows through the round contact, which can be done by calculating the Integral $I = \int_A \mathbf{j}\cdot\mathbf{df}$, where $A = \pi a^2$. So we have to integrate over the contact area, which means, that we can consider the current density in the z=0-plane, where the contact is a circle and μ is zero inside this circle (cf. figure 4).

In the contact area at z=0:

$$\mathbf{j}(\mu = 0) = -\frac{\sigma V}{a\pi\sin\nu}\hat{\mathbf{e}}_\mu \qquad (\text{at } \mu = 0,\ \hat{\mathbf{e}}_\mu = \hat{\mathbf{z}}\ ). \tag{12}$$

Because the current density doesn't depends on φ, we can write the current as $I = \int_0^a j(s)2\pi s\cdot ds$, where $s = \sqrt{x^2+y^2}$. Since it doesn't matter in which direction we integrate, we choose to perform the integration along the x-direction:

$$I = -2\pi\int_0^a \frac{\sigma V}{a\pi\sin\nu}x\cdot dx \tag{13}$$

We substitute: $x = a\cos\nu \quad dx = -a\sin\nu d\nu \qquad , \qquad 0 \to \frac{\pi}{2} \qquad a \to 0$

$$I = 2\pi\int_{\frac{\pi}{2}}^0 \frac{\sigma V}{a\pi\sin\nu}a^2\cos\nu\sin\nu d\nu = 2\sigma aV\left[-\sin(0) + \sin\left(\frac{\pi}{2}\right)\right] = 2\sigma aV \tag{14}$$

Finally we get the result of Maxwell using $V = R\cdot I$

$$\boxed{R = \frac{V}{I} = \frac{1}{2a\sigma} = \frac{\rho}{2a}} \tag{15}$$

with the resistivity ρ.

Now we want to apply these on the model for the 4-point-resistivity-measurement where we have the following situation:

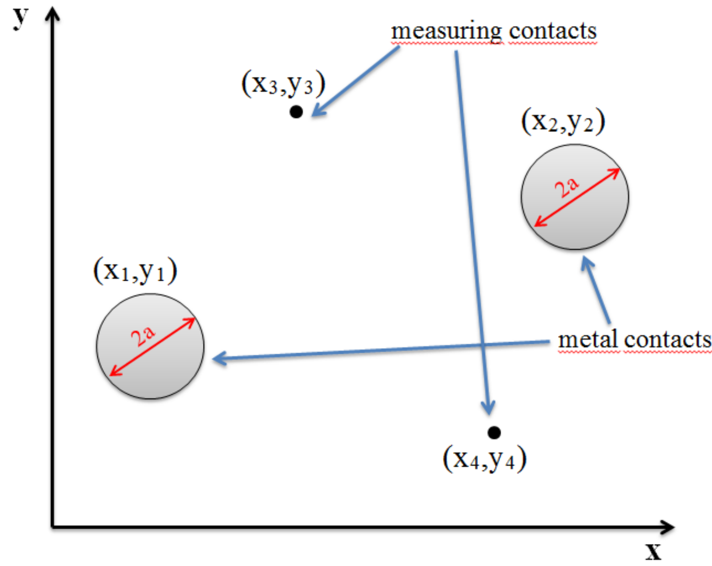

Figure 5: Configuration of the 4-point-resistivity-measurement: The current is injected on (x_1, y_1) and extracted on (x_2, y_2), where two metal contacts with the same diameter are positioned. The voltage is measured between (x_3, y_3) and (x_4, y_4).

The following idea is to calculate the voltage as difference of the electrostatic potential (8) between (x_3, y_3) and (x_4, y_4). First we calculate it just for the injection contact and then just for the extraction contact and then we add these two voltages together. For that we define the distances between the contacts as

$$s_{mn} = \sqrt{(x_m - x_n)^2 + (y_m - y_n)^2} \tag{16}$$

For the injection contact the differences to the measuring points are s_{31} and s_{41}, for the extraction contact they are s_{32} and s_{42}.

As already mentioned, ν is zero outside the metal contacts in the z=0-plane, so we can express μ as (cf. equation (1))

$$\mu = \cosh^{-1}\left(\frac{s}{a}\right) \tag{17}$$

Using equation (15), the electrostatic potential outside the metal contacts can be written as

$$\Phi_{mn} = \frac{I\rho}{a\pi} \cdot \tan^{-1}\left[\tanh\left(\frac{1}{2}\cosh^{-1}\left(\frac{s_{mn}}{a}\right)\right)\right] \tag{18}$$

To get the voltage between (x_3, y_3) and (x_4, y_4) we calculate the differences between the electrostatic potential for each contact and add them together:

$$\begin{aligned} V_{43} &= (\Phi_{41} - \Phi_{31}) - (\Phi_{42} - \Phi_{32}) \\ &= \frac{I\rho}{a\pi}\Bigg[\underbrace{\tan^{-1}\left[\tanh\left(\frac{1}{2}\cosh^{-1}\left(\frac{s_{41}}{a}\right)\right)\right]}_{v_{41}} - \underbrace{\tan^{-1}\left[\tanh\left(\frac{1}{2}\cosh^{-1}\left(\frac{s_{31}}{a}\right)\right)\right]}_{v_{31}} \\ &- \underbrace{\tan^{-1}\left[\tanh\left(\frac{1}{2}\cosh^{-1}\left(\frac{s_{42}}{a}\right)\right)\right]}_{v_{42}} + \underbrace{\tan^{-1}\left[\tanh\left(\frac{1}{2}\cosh^{-1}\left(\frac{s_{32}}{a}\right)\right)\right]}_{v_{32}}\Bigg] \end{aligned} \tag{19}$$

So finally we get the resistivity as

$$\boxed{\rho = \frac{a \cdot \pi \cdot V_{43}}{I \cdot (v_{41} - v_{31} - v_{42} + v_{32})}} \tag{20}$$

It would be interesting to apply that model on a measurement, where the contacts have a defined area. If the contact area goes to zero, the electric field and also the current density would diverge in that model (cf. equation 10 and 11), because the applied measuring current cannot flow through an infinite small area. The contact resistance in that model decreases by increasing the contact area (cf. equation 15).

Another interesting thing would be, to make a measurement configuration, in which the contact resistances can be measured. As mentioned at the beginning of this section, it should be advantageous to reduce the contact resistances of the inner contacts, where the voltage is measured. Here also round metal discs could be applied. So a configuration where 4 metal discs are deposited on a semiconductor surface and connected with a metal line, as shown in section 7, would be useful to test the model.

3.4 IV measurements

To characterize pn-junctions or Schottky contacts, IV curves are a useful tool. The IV curve is generated by applying a voltage between the measurement contacts and measuring the current flowing through the contacts. To get the current as a function of the voltage, the voltage is sweeped in a certain interval. (e.g. from $-10\,\mathrm{V}$ to $+10\,\mathrm{V}$) In our measurements we used as measuring contacts a tungsten tip, which is put on a silicon (or platinum) surface and on the other hand the copper contact on the edge of the investigated silicon sample. In such a case a typical Schottky characteristic as IV curve would be expected (cf. [16]).

4 Investigated Samples

4.1 Platinum Sample

As sample for the investigation of the platinum contacts, a p-doped silicon wafer (P570) was used. On the cross section of this wafer some platinum structures were deposited as shown in figure 6. The cross section was generated by scratching the wafer and breaking it along the (100)-direction. After that, the surface was ground. The resistivity of the silicon wafer was higher than 1000 Ω cm. There was about 15% oxygen and 70% carbon in the platinum. (These informations were given from the FELMI-ZFE [1], where the platinum structures were made.)
The platinum structures were made by EBID (Electron Beam Induced Deposition) [4, 13] at which 2 different set of parameters were used (pos1 and pos4 were generated different to pos2 and pos3). That should result in different efficiencies and electrical resistivities. Furthermore a difference between the structures could also be observed in figure 7, where pos1 and pos4 are a bit defocused and lightly blurred compared to the other two.
After a few measurements there was formed something like dust as it can be seen in figure 7.

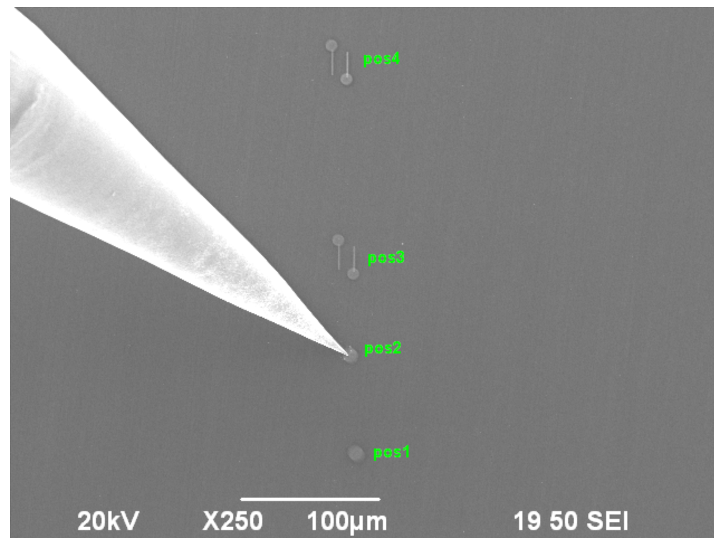

Figure 6: Platinum structures on the platinum sample: The SEM-picture shows the platinum structures, which were called pos1 – pos4. At pos1 and pos2 there are discs with a diameter of about 10 μm. At pos3 and pos4, two discs with a diameter of about 8 μm are positioned. On both of them a line with a length of 16 μm and width of 1 μm is attached. The distance between these lines is about 10 μm. All structures have a height of about 300 nm.

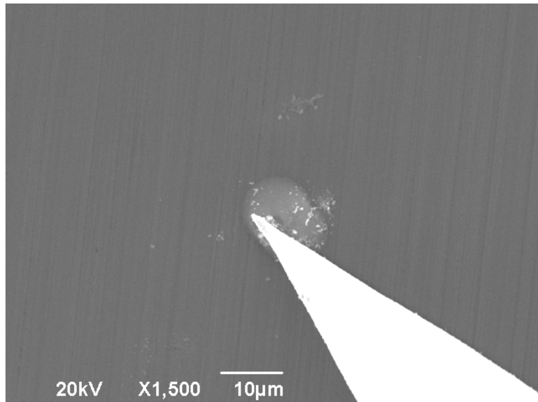

(a) pos1 with a tungsten tip on it (magnification = 1500, acceleration voltage = 20 kV). The structure is a bit defocused and blurred.

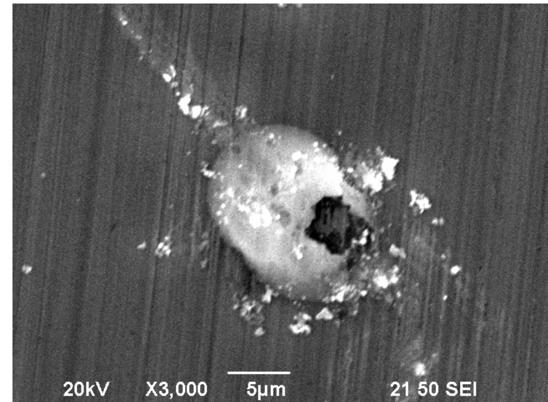

(b) pos1 after a few measurements (magnification: 3000, acceleration voltage: 20 kV). Here a destruction due to the landing of the tungsten tips can be observed.

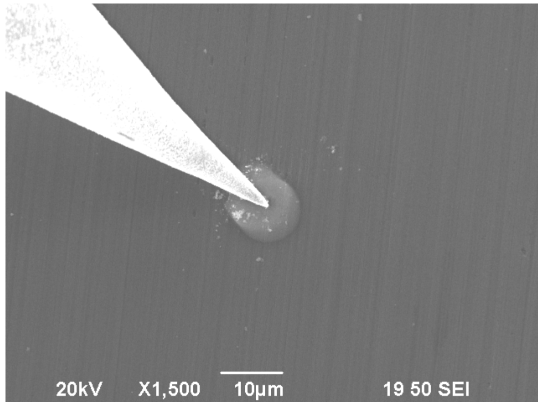

(c) pos2 with a tungsten tip on it (magnification = 1500, acceleration voltage = 20 kV). The structure is more focused.

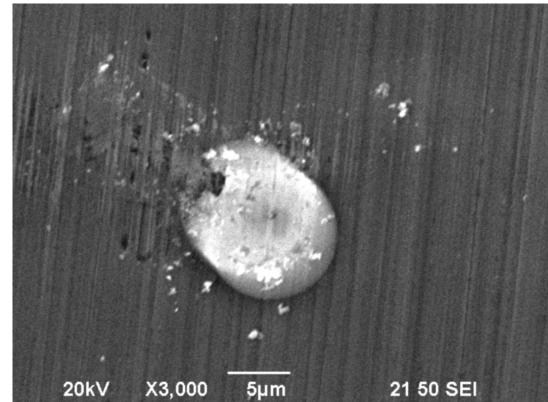

(d) pos2 after a few measurements (magnification: 3000, acceleration voltage: 20 kV). Here also a destruction can be observed.

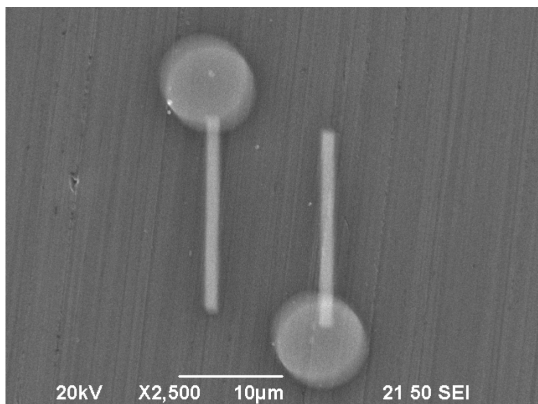

(e) pos3 (magnification: 2500, accerleration voltage: 20 kV), lightly defocused

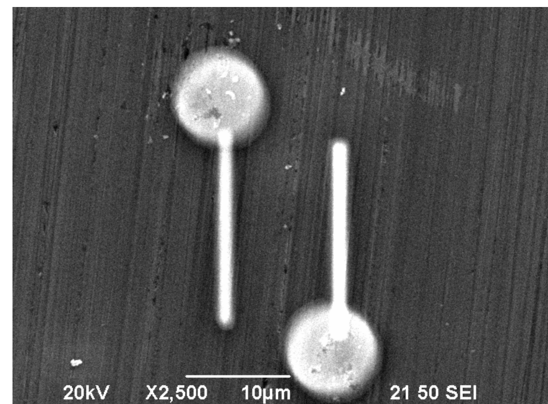

(f) pos4 (magnification: 2500, accerleration voltage: 20 kV), a bit more defocused

Figure 7: SEM pictures of the platinum structures deposited on sample 1. In the background some line structures, which come from the grinding process, can be observed.

4.2 EMCON Diode

As an example of a semiconductor power device (cf. section 2), an EMCON diode was investigated. The device consists of a thin p-doped layer and three different n-doped regions. The n-doped regions were generated by proton implantation. In that process positive charged hydrogen ions are accelerated into the specimen. During this process, defects are generated. After that the sample gets annealed, which causes that the defects are eleminated in the crystal lattice. In the end a n-doped region is generated, in which the size of the region depends on the penetration ability of the ions. [6, 7, 8, 10]

However, in the case of our EMCON sample, the regions of different doping concentrations were not known exactly. We made some EBIC measurements to figure out where the regions of different doping concentrations are. In figure 8 some EBIC scans are shown. The manufacturer of the device had expected, that the borders of the regions of different doping concentrations were 10 μm, 30 μm and 50 μm away from the right edge of the sample. In figure 8 (b) and (c) it can be seen, that there are three plateaus in the right half of the sample. These plateaus are separated by small peaks, which are the borders of the regions of different doping concentrations. They are about 10 μm, 30 μm and 50 μm away from the right edge, as the producer had expected.

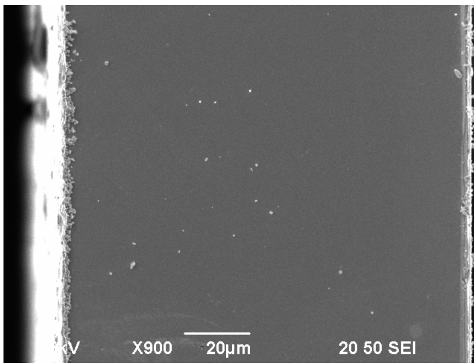

(a) SEM-picture of the EMCON diode, the figure shows the cross section of the device with a magnification of 900 and an acceleration voltage of 5 kV.

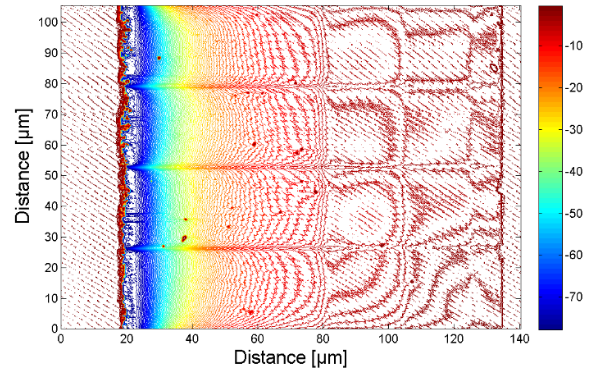

(b) EBIC measurement of the EMCON diode: The sample was contacted on the left and the right edge (measurement contacts), the figure shows the current flowing through the contacts as a 2D-map, on the right area the three regions of different doping concentrations can be observed, the 3 lines drawn over the sample come from EBIC linescans (cf. figure 8(c)).

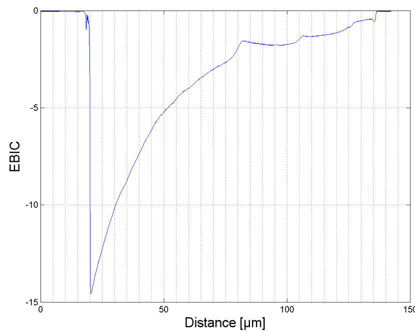

(c) EBIC linescan measurement: the 1D-doping profile can be observed with the pn-junction on the left side and the three different n-doped regions as plateaus on the right side.

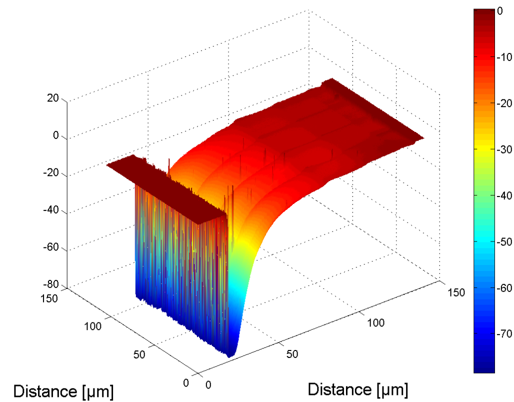

(d) EBIC scan of figure 8(b) as surface plot

Figure 8: EMCON diode: Seen from left to the right-hand side this EMCON diode consists of a thin boron doped layer followed by the pn-junction. To the right of the pn-junction the material is lightly n-doped. On the right side of the sample there are 3 regions of different doping concentrations which are generated by proton implantation. The first concentration step should be about 10 μm from the right edge of the sample, the next step should be about 30 μm and the last step about 50 μm away from the right edge.

5 Results

5.1 EBIC Measurements on the Platinum Sample

The EBIC measurements between a tungsten tip which touches the wafer directly and the edge contact of the sample yields the result, that the EBIC current has a maximum at the position of the measuring tip and decreases with rising distance to the tip. (see figure 1)

As mentioned in section 2, we expected that there is no EBIC current flowing at the regions of the platinum, because if the platinum was a good conductor there should not be generated charge carriers. With a simulation program (casino v2.42) we could show how the paths of the electrons from the e-beam look like if the beam hits the platinum. It turns out, that the e-beam goes through the platinum at an acceleration voltage of 20 kV, but it doesn't at 5 kV (cf. figure 9). At 20 kV more than 75% of the electrons don't penetrate the platinum.

So we expected to measure a very low EBIC current at the regions of the deposited platinum. That behavior can be seen in figure 11 (b), where there is no EBIC current measured at the platinum at 5 kV. In figure 11 (d) the same measurement is done with an acceleration voltage of 20 kV. There can be seen a EBIC current on one of the platinum pads. In figure 10 there was made an EBIC measurement between two tungsten tips, which are landed on the platinum discs of pos3. This measurement doesn't show the expected behavior.

We also compared the EBIC measurements with a tip on silicon and with a tip on the platinum. A result can be observed in figure 12. There was also measured an EBIC current at the platinum regions. In the case where the measuring tip is landed on a platinum pad, the EBIC signal area is much larger than if it's landed on silicon.

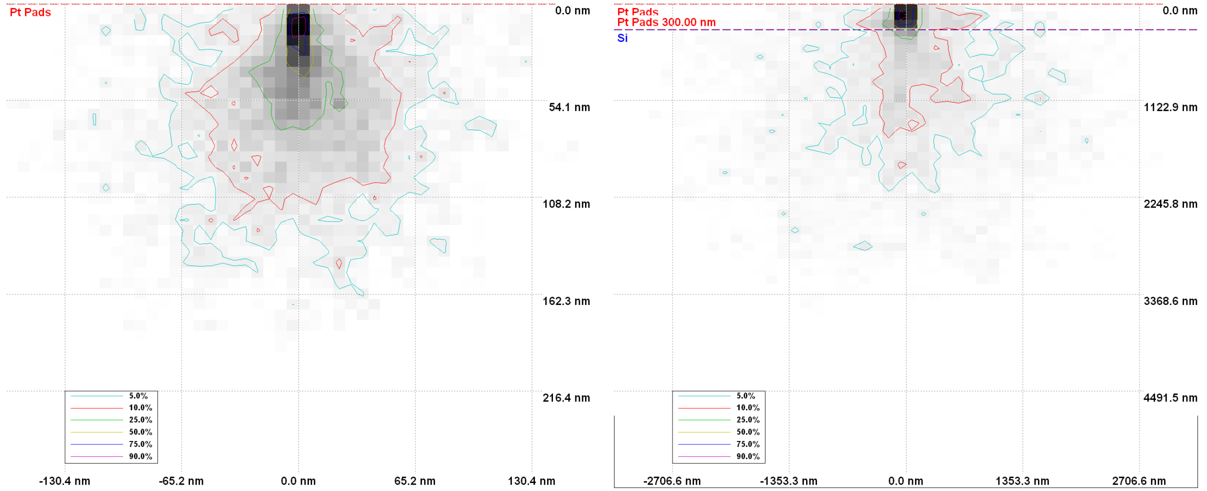

(a) With an acceleration voltage of 5 kV the penetration depth is only about 160 nm, so the electrons cannot go through the platinum structures.

(b) With an acceleration voltage of 20 kV the penetration depth in platinum is about 2000 nm, but more than 75% of the electrons don't go through the about 300 nm high platinum.

Figure 9: Simulation of the energy distribution of the e-beam in platinum. The calculation was done for 15% platinum with 70% carbon and 15% oxygen.

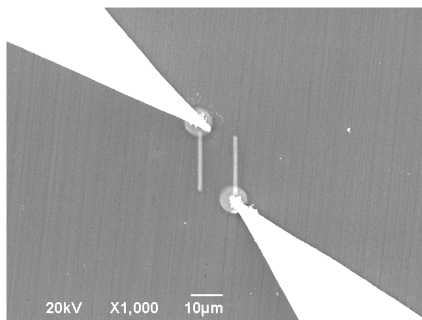

(a) SEM picture: the tips are landed on pos3 (magnification: 1000, acceleration voltage: 20 kV).

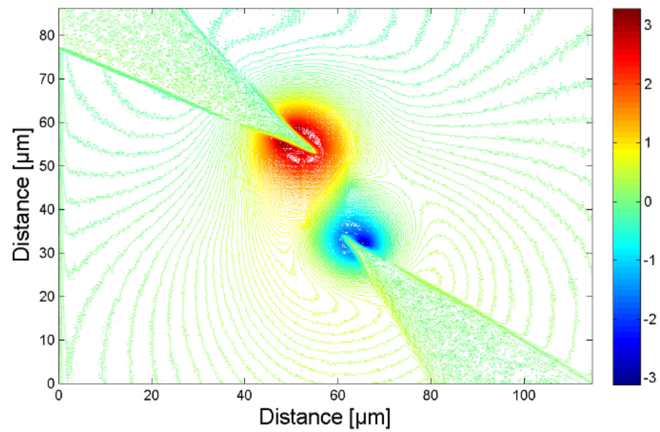

(b) The EBIC current was measured between the 2 tips. Against our expectations, there is measured an EBIC current at the regions of the platinum. If there aren't deposited any platinum structures, the result should be almost the same.

Figure 10: EBIC measurement: between 2 tips on pos3 (the measuring tip is on the right structure)

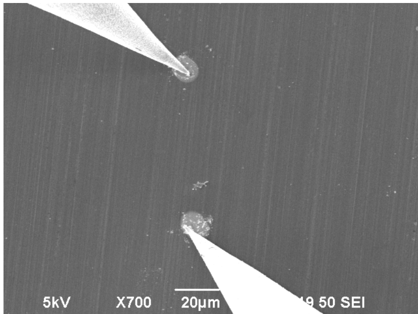

(a) SEM picture: the measuring tips are landed on pos1 and pos2 (magnification: 700, acceleration voltage: 5 kV).

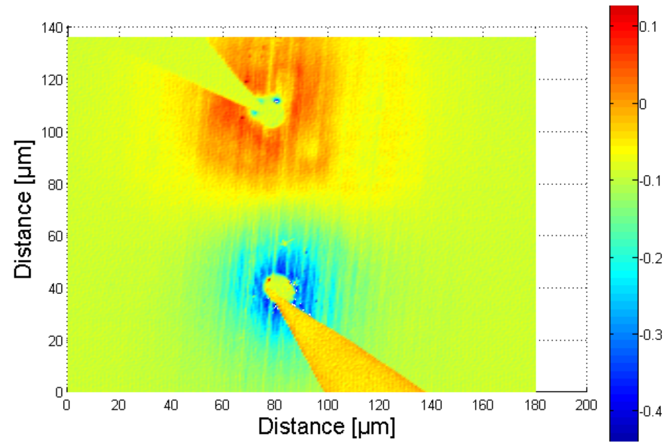

(b) At this acceleration voltage it can be seen, that the e-beam doesn't penetrate through the platinum.

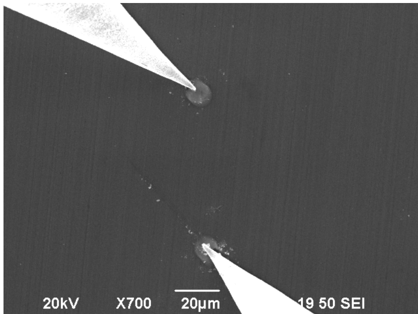

(c) SEM picture: the measuring tips are landed on pos1 and pos2 (magnification: 700, acceleration voltage: 20 kV).

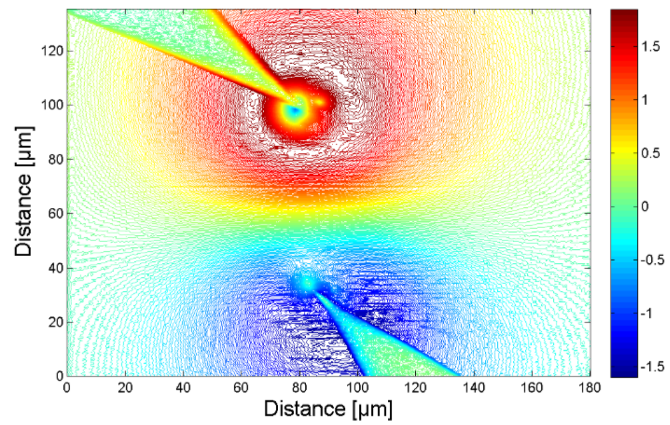

(d) Here the e-beam penetrates through at pos1.

Figure 11: EBIC measurement: between 2 tips on pos1 and pos2 (the measuring tip is on pos1)

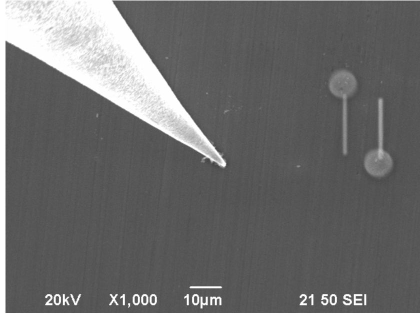

(a) SEM picture: the measuring tip is landed on the sample beside pos4 (magnification: 1000, acceleration voltage: 20 kV).

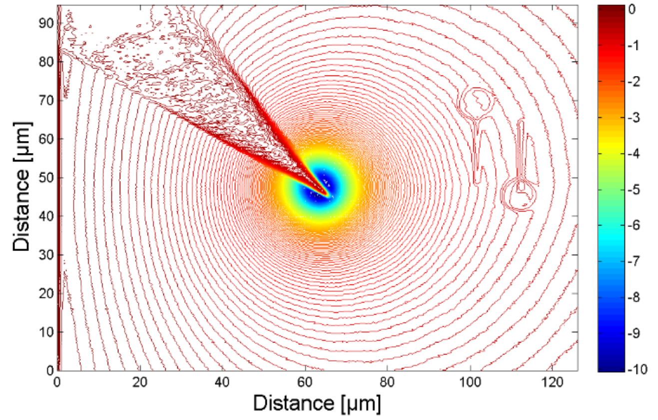

(b) The measurement shows the typical current 2D-map if the measuring tip is put on a p-doped sample.

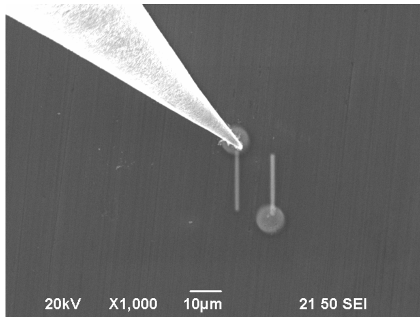

(c) SEM picture: the measuring tip is landed on the left platinum disc of pos4 (magnification: 1000, acceleration voltage: 20 kV).

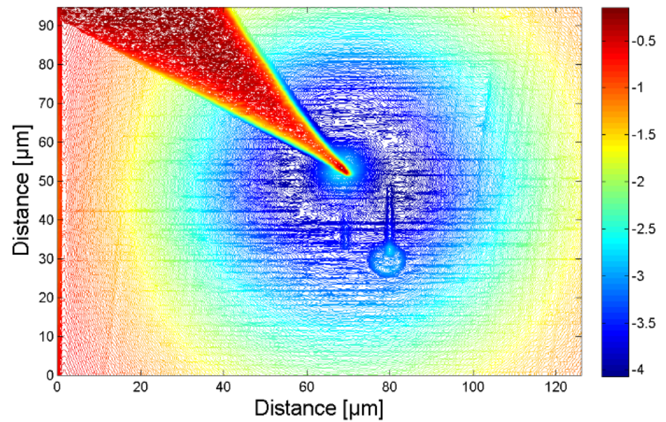

(d) Measuring tip on the platinum: against the expectations the EBIC current is not close to zero on the platinum. Moreover the large diffusion length is strange.

Figure 12: EBIC measurement: Comparison of silicon and platinum at pos4. The EBIC measurements were done with an acceleration voltage of 20 kV.

The EBIC measurements indicate, that the deposited platinum doesn't show the properties of an ideal metal. Moreover there was an increasing of the diffusion length, which we couldn't explain (see e.g. figure 12). In the progress of our measurements we also noticed, that there was built something like dust on the platinum discs, as it can be observed in figure 7 (a) - (d).

5.2 Resistance of the Platinum

We measured the resistance of the platinum by landing two tips on one platinum pad as shown in figure 13 (a). With a source meter (KEITHLEY 2636A) we measured the resistances at different applied voltages between the tips. The same measurement we did for silicon by landing two tips on the surface of the probed wafer. The distance between the measuring tips was about the same as it was on the platinum pad. (cf. figure 13 (b)) The measured values are shown in table 1. These values only indicate the magnitude of the resistances (it's not useful to present the exact values, because the measurements depend inter alia on how good the contact is).

Table 1: Resistance Comparison between Platinum and Silicon

The resistances were measured with the sourcemeter between two tips which were landed on platinum respectively on silicon. The values should show the magnitude of the resistances.

applied voltage	resistance of the platinum	resistance of the silicon
[V]	[MΩ]	[MΩ]
1	1.0	100
0	0.5	100
-1	1.0	100

In general it can be seen, that the resistance of the platinum is about 2 magnitudes lower than the resistance of the silicon, which has a resistivity of more than 1000 Ωcm. The resistivity of pure platinum is about 10^{-5} Ωcm. The high resistance of the deposited platinum indicates, that this platinum is no ideal metal (an ideal metal would have a resistance in the magnitude of a few Ω). One reason for the high resistance could be the influence of the carbon and oxygen in the deposited platinum [4]. We assume, that the measured resistance could also depend on how homogeneous the platinum is. That means, that certain spots of high resistivities would influence the measurement. So it would be interesting to make the measurement arrangement as described in section 7, where two platinum pads are connected by a platinum line.

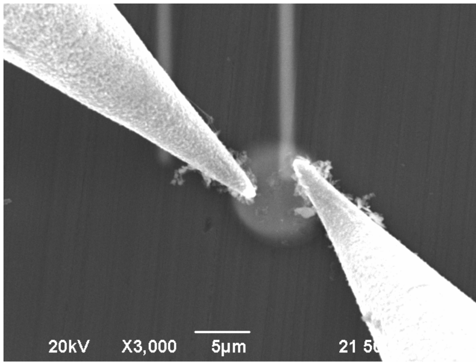

(a) SEM picture of two tungsten tips which are landed on the right platinum disc of pos4 (magnification: 3000, acceleration voltage: 20 kV).

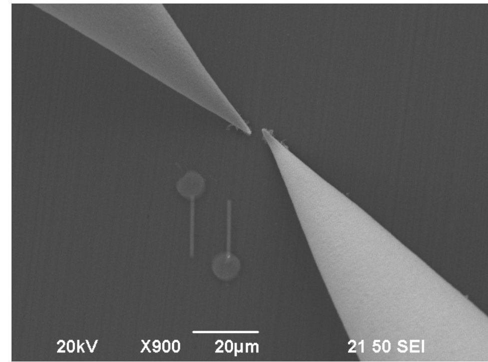

(b) SEM picture of two tungsten tips which are landed close together on the silicon surface beside pos4 (magnification: 900, acceleration voltage: 20 kV).

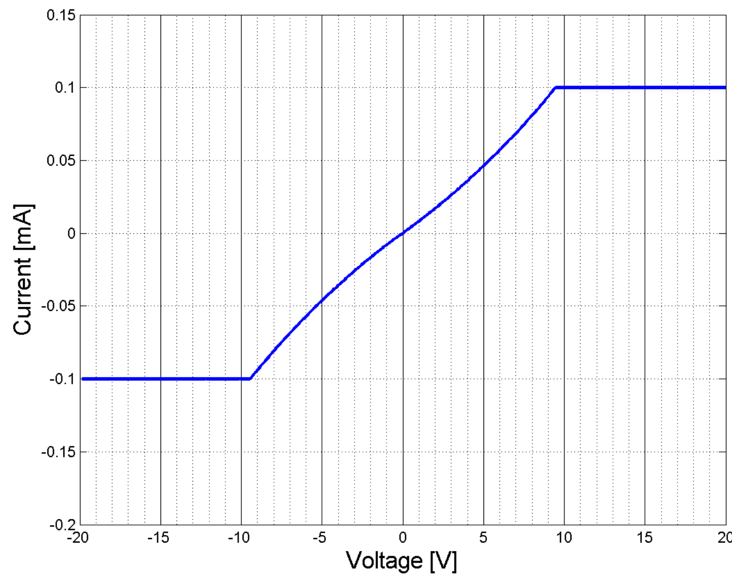

(c) IV-curve recorded from -20 V to 20 V, the measuring tips were landed on one platinum pad as shown in figure 13 (a).

Figure 13: Resistance measurements: Two tungsten tips are landed on the investigated material with a distance of about 5 μm.

In figure 13 (c) a IV-curve, recorded from -20 V to 20 V is shown. The horizontal lines indicates the saturation of the measuring device. In between the current increases with rising voltage, but it's not a straight line, as it would be by an ideal metal. So the IV curve also shows, that the deposited platinum is no ideal metal.

We also wanted to investigate the influence of the e-beam on the deposited platinum. Since the emission current [5] depends on the acceleration voltage, the spot size and the alignment of the filament, we first made a filament alignment. Then we landed two tips on one platinum pad and zoomed in with the microscope in the way, that the screen was totally filled with the investigated platinum pad (cf. figure 14 (a) and (b)). This should increase the influence of the e-beam on the platinum disc. Then we biased the tips with 1 V and measured the resistance of the platinum. To show the influence of the e-beam, first we blanked the beam for a minute, which means, that the e-beam gets distracted by applying a voltage. Then we switched off the blanking for about 11 minutes and after that we blanked the beam again for about one minute. This measurement we first did with an acceleration voltage of 5 kV and then we did it again with an acceleration voltage of 20 kV.

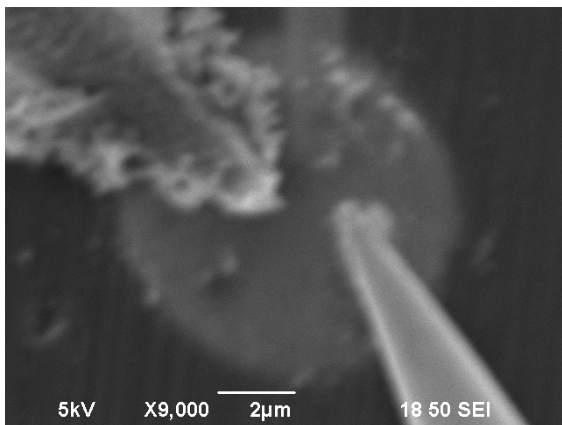

(a) SEM picture of the measurement situation with an acceleration voltage of 5 kV and a magnification of 9000. The two tungsten tips are landed on the right pad of pos4.

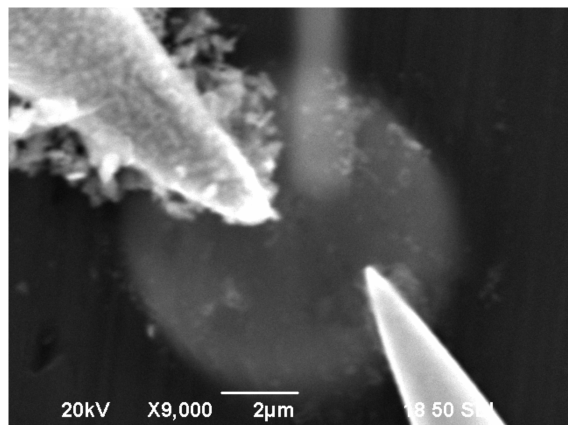

(b) SEM picture of the measurement situation with an acceleration voltage of 20 kV and a magnification of 9000. The two tungsten tips are landed on the right pad of pos4.

Figure 14: Resistance as a function of time: SEM pictures of the measuring situation

The results of the measurement can be seen in figure 15. For an acceleration voltage of 5 kV the resistance was in the region of 100 kΩ. When the e-beam wasn't blanked, the resistance doesn't change considerably, maybe a little decreasing can be observed. For an acceleration voltage of 20 kV the resistance was in general in the region of about 13 kΩ, so it was lower than at the measurement with 5 kV. At 20 kV a noticeable influence of the e-beam can be considered. The resistance starts to decrease continuously when the e-beam hits the platinum. The manufacturer of the platinum structures mentioned, that the reason for the registered influence of the e-beam could be, that the e-beam breaks the included carbon out of the platinum. Also it should be mentioned, that the measuring signal was more stable at 20 kV. That might has to do with the contact stability.

Generally the measurements indicate an influence of the e-beam on the deposited platinum.

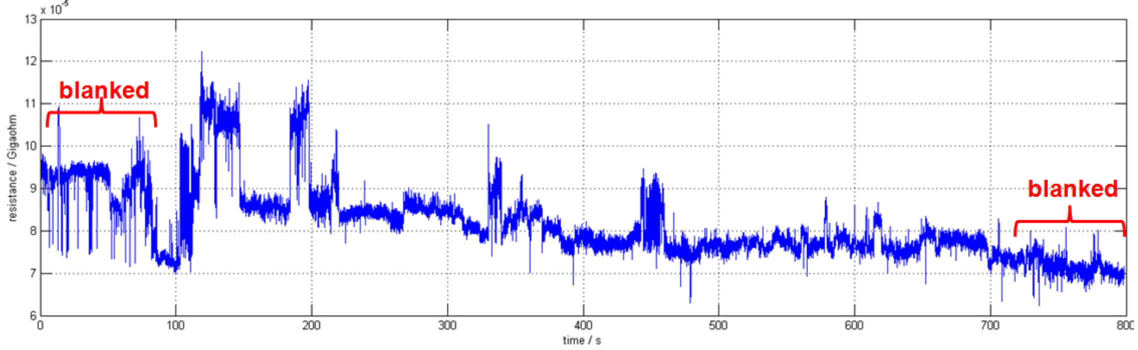

(a) The resistance was measured as a function of time at an acceleration voltage of 5 kV. For the first and the last minute the e-beam was blanked.

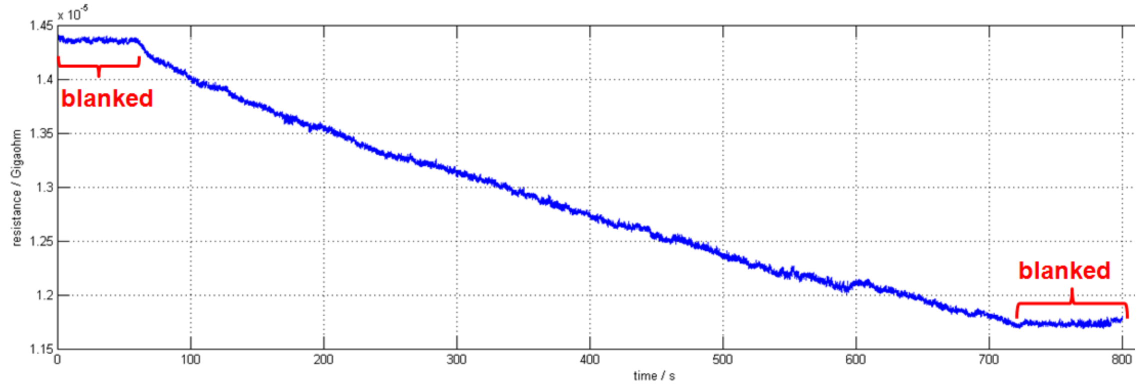

(b) The resistance was measured as a function of time at an acceleration voltage of 20 kV. For the first and the last minute the e-beam was blanked.

Figure 15: Resistance as a function of time measured at acceleration voltages of 5 kV and 20 kV

5.3 Stability of the Contacts

We also investigated the stability of the platinum contacts. Therefore we landed a tungsten tip on a platinum disc and applied a voltage of 5 V between the tip and the edge of the probed sample, while we measured the current flowing from the tip trough the sample to the edge contact of the sample. The measuring current was amplified by a current amplifier (SRS model sr570). To get only the noise signal of the contact, we filtered the measuring signal (high frequency filter) with the amplifier and we also corrected the current offset. With a LabView program, the output voltage signal of the amplifier was recorded as a function of time. We repeated the same measurement, the

first time by landing the tip onto another platinum pad, and the next two times by putting a measuring tungsten tip on the silicon surface of the sample. In figure 16 the four measurement curves can be seen. For the last measurement we put a worn and therefore more bent tip (tip4) on the silicon surface. That contact should be a bit more unstable than the contacts with the sharp measuring tip (tip1).

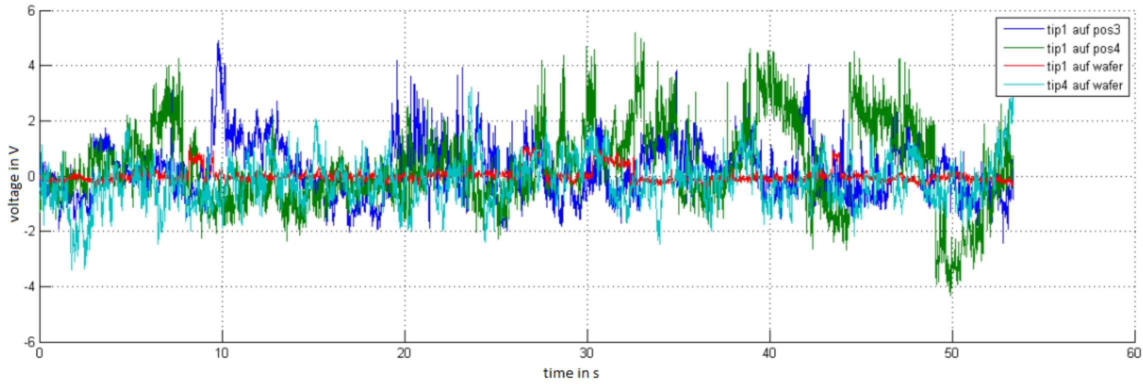

Figure 16: Stability of the contacts: the 4 measuring signals indicate the stability of the several contacts. The diagram shows the voltage as a function of time. The dark blue line is the measuring signal, where the tungsten tip was landed on the platinum pad on pos3, the green curve is the measuring signal of the same tip landed on the platinum disc on pos4, the red line comes from the measurement, where the same tip was landed on silicon, and the light blue curve is the signal, where another tip (tip4) was landed on silicon.

By observing the results, it is obviously that the noise signal measured with the tip on the platinum pads is much larger than the other two. That means, that the contact of the tungsten tip on the silicon is more stable than the contact, where the tungsten tip touches the deposited platinum. We also calculated the standard deviations of the current signals to underline the results.

tungsten tip1 on Pt at pos3 $\rightarrow \sigma = 1.013\,\text{nA}$
tungsten tip1 on Pt at pos4 $\rightarrow \sigma = 1.466\,\text{nA}$
tungsten tip1 on Si $\rightarrow \sigma = 0.244\,\text{nA}$
tungsten tip4 on Si $\rightarrow \sigma = 0.850\,\text{nA}$

5.4 IV Curves

To investigate the characteristic of the platinum contacts in comparison with silicon we finally made some IV-measurements. We landed a tungsten tip on the platinum pad

and recorded an IV curve, in which the measuring contacts was the tungsten tip on the one hand and the edge of the silicon on the other hand. Then we landed the tip on the silicon surface and did the same measurement again. For the IV measurements we used a program (TSP), which applied the voltage and measured the current with using a sourcemeter (KEITHLEY 2636A). The results are shown in figure 17.

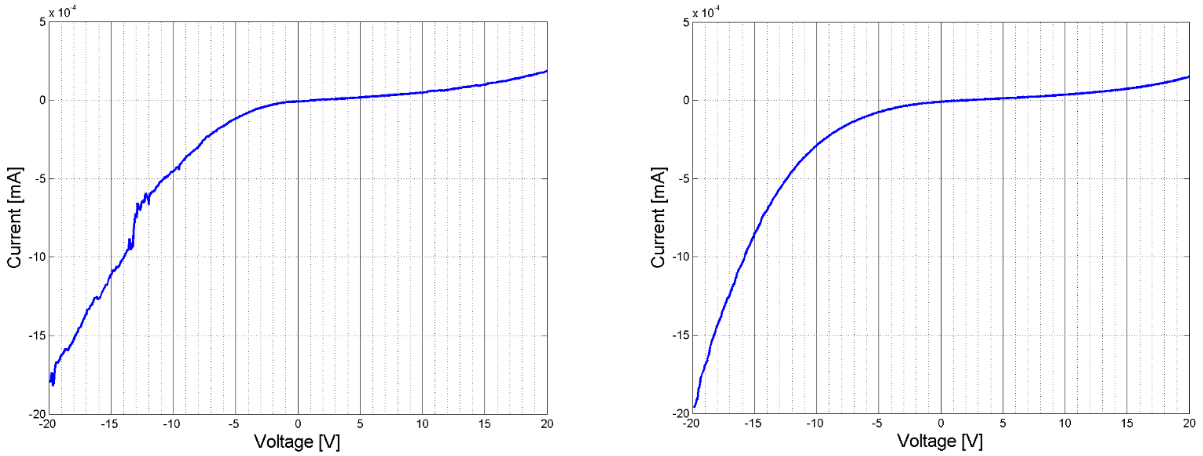

(a) The measuring tip was landed on a platinum pad at pos4.

(b) The measuring tip was landed on silicon beside pos4.

Figure 17: IV curves: comparison Pt vs. Si. The voltage was applied from -20 V to 20 V.

The IV curves show a smooth line in the case of silicon (like a usual double Schottky curve). In the case of platinum the left region was very unstable. So the comparison shows, that the platinum Schottky contact is not as useful as the case, where the tungsten tip is directly landed on the silicon.

6 Conclusions

This bachelor thesis considered, if the electron beam induced current deposited platinum pads are suitable as stable and reproducible Schottky contacts with a defined contact area. The expectations for these platinum pads were, that the contact resistance should be reduced because of the large contact area. We assumed, that the deposited platinum should be a quite good conductor, to get a well defined Schottky contact. However, the experiments we made during this project have shown, that the deposited platinum is far from an ideal metal. The manufacturer of the platinum structures confirmed, that the platinum includes 70% of carbon and 15% of oxygen, which could be responsible for the bad resistance of the platinum (cf. section 5.2). Otherwise, the reason also could be local clusters of the inclusions, so it would be interesting to investigate the homogeneity of the platinum.

The stability measurements also indicate, that the platinum contacts were more unstable, than the contact where the tungsten needle was directly landed on the silicon surface (cf. section 5.3). This was confirmed by making some IV curves of the platinum contacts in comparison with the direct tungsten contact, which for example can be seen in figure 17.
Another interesting aspect was shown, when we measured the resistance as a function of time in dependence of the electron beam. It seams, that there was a "curing" process during the e-beam falls on the platinum. These effect was more significant at higher beam energies (cf. figure 15).

In summary the measurements have shown, that the deposited platinum structures were not suitable as Schottky contacts in that case. However, it would be interesting to search for the reasons of the problems, as there was the stability and the resistance of the platinum. It could also be possible, that these problems have to do with the platinum-silicon interface. We are not sure, if the surface was really clean before the EBID process. It could be better only to break the sample without grinding. Maybe also a cleaning process could be made before depositing the platinum.

7 Suggestions

- As mentioned in section 6 it might be interesting to make another sample with deposited platinum structures, where the surface was cleaned before the deposition process.
- For the resistance measurements, but also for 4-point resistivity measurements it would be convenient to have platinum patterns as shown in the figure below. The pattern on the left hand side, which would be used for the resistance measurement, should be deposited on an insulating substrate. With two tungsten tips landed on different positions of the structure, it should be possible to measure the resistance as a function of the position. That would give an information about the homogeneity of the platinum.

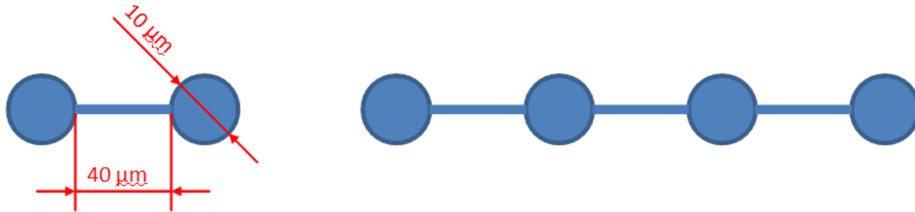

- It would be interesting to apply the model for the 4-point measurement on metal discs as shown in figure 5. To get well defined round metal current contacts, maybe it would be advantageous to try depositing other materials like gold.

List of Figures

1 EBIC measurement between a tungsten tip and a p-doped silicon wafer . 6
2 2-point Measurement 7
3 4-point Measurement 8
4 Oblate spheroidal coordinates in the x-z-plane 10
5 Configuration of the 4-point-resistivity-measurement 13
6 Platinum structures on the platinum sample 16
7 SEM pictures of the platinum structures deposited on the platinum sample 17
8 EBIC measurements of an EMCON diode 19
9 Simulation of the energy distribution of the e-beam in platinum 21
10 EBIC measurements: between 2 tips on pos3 21
11 EBIC measurements: between 2 tips on pos1 and pos2 22
12 EBIC measurement: Comparison of silicon and platinum at pos4 23
13 Resistance measurements 25
14 Resistance as a function of time: SEM pictures 26
15 Resistance as a function of time 27
16 Stability of the contacts: the 4 measuring signals indicate the stability of the several contacts 28
17 IV curves: comparison Pt vs. Si 29

References

[1] Institute for Electron Microscopy and Fine Structure Research (FELMI) of Graz University of Technology and the Graz Centre for Electron Microscopy (ZFE Graz) which is held by the Verein zur Foerderung der Elektronenmikroskopie und Feinstrukturforschung. http://www.felmi-zfe.tugraz.at/.

[2] Date: 17.07.2012. Stick-slip phenomenon. Website. http://en.wikipedia.org/wiki/Stick-slip_phenomenon.

[3] Date: 25.07.2012. Four point resistivity measurements. Website. http://lamp.tu-graz.ac.at/~hadley/sem/4pt/4pt.php.

[4] Date: 26.07.2012. Electron beam-induced deposition. Website. http://en.wikipedia.org/wiki/Electron_beam-induced_deposition.

[5] Date: 26.07.2012. Emission current. Website. http://lamp.tu-graz.ac.at/~hadley/sem/faraday/faraday.php.

[6] Date: 26.07.2012. Ionenimplantation. Website. http://de.wikipedia.org/wiki/Ionenimplantation.

[7] Radiation Damage in Silicon Particle Detectors-microscopic defects 3. M. Moll and (1999) macroscopic properties, Ph.D. thesis.

[8] Ph.D. thesis (2011) A. Junkes, Influence of radiation defect clusters on silicon particle sensors.

[9] P. Eyben, T. Janssens, and W. Vandervorst. Scanning spreading resistance microscopy (SSRM) 2d carrier profiling for ultra-shallow junction characterization in deep-submicron technologies. *Materials Science and Engineering*, B 124-125:45–53, (2005).

[10] J. Hartung and J. Weber. Defects created by hydrogen implantation into silicon. *Materials Science and Engineering*, B4:pp. 47–50, (1989).

[11] Martin Kupper. Very Sharp Platinum Tips by Electrochemical Etching. *Graz University of Technology*, (2012).

[12] J. C. Maxwell. A Treatise on Electricity and Magnetism. *Clarendon Press*, Oxford (1904).

[13] Kazutaka Mitsuishi. *Nanofabrication.* World Scientific Publishing Co. Pte. Ltd., (2008). Chapter 11.

[14] P. Reuter, T. Rath A., Fischereder, G. Trimmel, and P. Hadley. Electron Beam-Induced Current (EBIC) in Solution-Processed Solar Cells. *Wiley Periodicals, Inc.*, Volume 33, (2011).

[15] Paul G. Slade. Electrical Contacts. *Marcel Dekker, Inc.*, pages 1 – 7, 1999.

[16] G. D. J. Smit, S. Rogge, and T. M. Klapwijk. Enhanced tunneling across nanometer-scale metal-semiconductor interfaces. *APPLIED PHYSICS LETTERS*, Volume 80, (2002).